Carbohydrate Polymers 157 (2017) 128–136

Contents lists available at ScienceDirect

Carbohydrate Polymers

journal homepage: www.elsevier.com/locate/carbpol

The polysaccharide and low molecular weight components of *Opuntia ficus indica* cladodes: Structure and skin repairing properties

Flaviana Di Lorenzo[a], Alba Silipo[a], Antonio Molinaro[a], Michelangelo Parrilli[b], Chiara Schiraldi[c], Antonella D'Agostino[c], Elisabetta Izzo[c], Luisa Rizza[d], Andrea Bonina[d], Francesco Bonina[e], Rosa Lanzetta[a,*]

[a] Department of Chemical Sciences, University of Naples Federico II, Via Cintia 4, I-80126 Napoli, Italy
[b] Department of Biology, University of Naples Federico II, Via Cintia 4, I-80126 Napoli, Italy
[c] Department of Experimental Medicine, Second University of Naples, via de Crecchio 7, I-80138 Napoli, Italy
[d] Bionap srl, R&D Contrada Fureria, ZIO 950125 Piano Tavola, Belapsso, Italy
[e] Department of Drug Sciences, University of Catania, Catania, Italy

ARTICLE INFO

Article history:
Received 27 July 2016
Received in revised form
15 September 2016
Accepted 23 September 2016
Available online 24 September 2016

Keywords:
Opuntia ficus-indica
Cladodes mucilage
Polysaccharide
Wound-healing assay
Cicatrizing property

ABSTRACT

The *Opuntia ficus-indica* multiple properties are reflected in the increasing interest of chemists in the identification of its natural components having pharmaceutical and/or cosmetical applications. Here we report the structural elucidation of *Opuntia ficus-indica* mucilage that highlighted the presence of components differing for their chemical nature and the molecular weight distribution. The high molecular weight components were identified as a linear galactan polymer and a highly branched xyloarabinan. The low molecular weight components were identified as lactic acid, D-mannitol, piscidic, eucomic and 2-hydroxy-4-(4′-hydroxyphenyl)-butanoic acids. A wound healing assay was performed in order to test the cicatrizing properties of the various components, highlighting the ability of these latter to fasten dermal regeneration using a simplified *in vitro* cellular model based on a scratched keratinocytes monolayer. The results showed that the whole *Opuntia* mucilage and the low molecular weight components are active in the wound repair.

1. Introduction

In traditional medicine, herbs and plants containing mucilage, polysaccharides and starch are widely employed in relieving skin epithelium wound and mucosal irritation (Trombetta et al., 2006). Nowadays, skin wound-healing and repairing effects have been demonstrated for some of traditionally used herbs, such as *Calendula officinalis* (Parente et al., 2012), *Malva silvestris* (Pirbalouti, Azizi, Koohpayeh, & Hamedi, 2010), *Typha latifolia* (Gescher & Deters, 2011). The beneficial effects in promoting skin repair have been observed on various phases of wound-healing such as in bioadhesive ability, immunomodulation, cell–cell and cell-matrix interactions and collagen synthesis (Gescher & Deters, 2011; Parente et al., 2012; Pirbalouti et al., 2010).

The prickly pear cactus *Opuntia ficus-indica* (L.) is a tropical and subtropical plant able to grow in arid climates, such as the Mediterranean and Central America regions. It has recently received an ever increasing attention from researchers worldwide for its multivalent pharmaceutical and cosmetical potential (Kaur, Kaur, & Sharma, 2012; Rizza, Frasca, Nicholls, Puglia, & Cardile, 2012; Trombetta et al., 2006). Cladodes are particularly rich in carbohydrate-containing polymers, known as mucilage, made up of several sugar residues such as arabinose, galactose, rhamnose, xylose and galacturonic acid (Sepúlveda, Sáenz, Aliaga, & Aceituno, 2007). It has been previously reported that polysaccharides from *Opuntia* plants can be used as mucoprotective agents due to their capability to form a molecular network and to retain huge amount of water. Thus, they can act as a protective layer on mucosal surfaces accelerating the re-epithelization of dermal wound (Galati, Monforte, Tripodo, d'Aquino, & Mondello, 2001; Galati, Pergolizzi, Miceli, Monforte, & Tripodo, 2002; Kaur et al., 2012). In this context, Trombetta et al. (2006) demonstrated that

Abbreviations: OPF, *Opuntia* polysaccharide fraction; ORE, *Opuntia* Rough extract; OSMF, *Opuntia* small molecular weight fraction.

* Corresponding author.
E-mail addresses: flaviana.dilorenzo@unina.it (F. Di Lorenzo), silipo@unina.it (A. Silipo), molinaro@unina.it (A. Molinaro), parrilli@unina.it (M. Parrilli), chiara.schiraldi@unina2.it (C. Schiraldi), antonella.dagostino@unina2.it (A. D'Agostino), elisabetta.izzo@unina2.it (E. Izzo), luisa.rizza@bionap.com (L. Rizza), andrea.bonina@bionap.com (A. Bonina), boninaf@gmail.com (F. Bonina), lanzetta@unina.it (R. Lanzetta).

http://dx.doi.org/10.1016/j.carbpol.2016.09.073
0144-8617/

topical application of polysaccharides from *Opuntia* cladodes on skin lesions in rats can accelerate the re-epithelization by affecting cell-matrix interactions and by modulating laminin laying, owing to their peculiar hygroscopic, rheological and viscoelastic properties. Moreover, polysaccharides isolated from *Opuntia* cladodes have highlighted an interesting and remarkable bio-adhesive effect on mucosal surface in some *in vitro* cell models (Rizza et al., 2012). However, previous studies have been focused only on the purified polysaccharide fraction from *Opuntia* cladodes thus no information has been reported to date about the whole extract and other non-carbohydrate components. Thus, to the best of our knowledge, very little is known about the structure-activity relationship between above described skin wound-healing effects and the cladode mucilage molecular composition.

Here we report the complete structural characterization of the polysaccharide and non-polysaccharide low molecular weight components from *Opuntia ficus-indica* (L.) (referred to here on as *Opuntia*) cladodes mucilage. The repairing activity of the isolated components was also evaluated by an innovative cell model mimicking *in vivo* conditions.

2. Materials and methods

2.1. Samples preparation

Opuntia cladode extract was supplied by BIONAP srl (OPUNTIA BIOCOMPLEX SH, Italy). *Opuntia* cladode juice was extracted by a mechanically press system and lyophilized to obtain a powder containing *Opuntia* mucilage (ORE). Thereafter, a weighted amount of ORE was dissolved in water (0.5% w/w) and purified by ultrafiltration system, equipped with a semi-permeable PES (polyethersulfone) membrane (KMS HFK^{TM} – 131, Koch, USA) with a cut-off of 10 kDa. This process gave two fractions containing small molecular components (OSMF) and high molecular weight polysaccharides (OPF) respectively.

2.2. Chemical analyses on the Opuntia polysaccharide fraction (OPF)

Determination of the sugar residues by gas-liquid chromatography/mass spectrometry (GLC–MS) analysis was carried out as previously described (De Castro, Parrilli, Holst, & Molinaro, 2010; Leontein & Lönngren, 1978). Monosaccharides were detected as acetylated *O*-methyl glycoside derivatives. After methanolysis (1.25 M HCl/MeOH, 85 °C, 24 h) and acetylation with acetic anhydride in pyridine (85 °C, 30 min), the sample was analyzed by GLC–MS. The absolute configuration of sugar residues has been established by GLC–MS analysis of the acetylated *O*-(+)-2-octyl glycosides derivatives and comparison with authentic standards. Linkage analysis was performed by methylation of the complete saccharide portion as described elsewhere (Ciucanu & Kerek, 1984; De Castro et al., 2010); the sample was methylated with iodomethane, hydrolyzed with trifluoroacetic acid (2 M, 100 °C, 2 h), carbonyl-reduced with sodium tetradeuteroborate ($NaBD_4$), acetylated with acetic anhydride and pyridine, and analyzed by GLC–MS. An aliquot of OPF was treated for 48 h with α-amylase from *Aspergillus oryzae* (Sigma-Aldrich A6211) and dialyzed exhaustively against distilled water. The digested product was collected, lyophilized and underwent above mentioned chemical analyses and further analyzed by NMR spectroscopy. An aliquot of the OPF was also treated with hydrofluoric acid (HF) (40%) for 48 h at 4 °C and dialyzed. The product was then purified by gel-filtration chromatography and the fractions obtained were analyzed by NMR spectroscopy.

2.3. Purification and separation of the Opuntia small molecules fraction (OSMF)

20 mg of the lyophilized OSMF were injected into a 1.5 × 120 cm Bio-Gel P-2 Extra Fine packed column (the useful fractionation range for carbohydrate and small peptide separations is 100–1800 Da, according to Bio-Rad). Gel filtration chromatography was run at room temperature with a flow rate of 8 cm/hr, using distilled and degassed water as eluent. The four fractions of 1.8 mL were collected, lyophilized and analyzed by NMR spectroscopy. The column was calibrated using Bio-Rad's Gel Filtration Standards having known relative molecular weights ranging from 600 kDa to 1 kDa.

2.4. NMR spectroscopy analysis

1D and 2D ^{1}H NMR spectra were recorded in D_2O at 300 K at pD = 7 with a Bruker 600 DRX spectrometer equipped with a cryo-probe. The spectra were calibrated with internal acetone ($\delta H = 2.225$ ppm; $\delta C = 31.45$ ppm). Total correlation spectroscopy (TOCSY) experiments were performed with spinlock times of 100 ms by using data sets (t1 × t2) of 4096 × 256 points. Rotating frame Overhauser enhancement spectroscopy (ROESY) and Nuclear Overhauser enhancement spectroscopy (NOESY) experiments were performed by using data sets (t1 × t2) of 4096 × 256 points with mixing times between 100 and 400 ms, acquiring 16 scans. Double-quantum-filtered phase sensitive correlation spectroscopy (DQF-COSY) experiments were executed by using data sets of 4096 × 512 points. The data matrix in all the homonuclear experiments was zero-filled in both dimensions to give a matrix of 4 K × 2 K points and was resolution-enhanced in both dimensions by a cosine-bell function before Fourier transformation. Coupling constants were determined by 2D phase-sensitive DQF-COSY (Piantini, Sorensen, & Ernst, 1982; Rance et al., 1983), Heteronuclear single quantum coherence (HSQC) and heteronuclear multiple bond correlation (HMBC) experiments were executed in ^{1}H-detection mode by single-quantum coherence with proton decoupling in the ^{13}C domain using data sets of 2048 × 256 points. HSQC was carried out using sensitivity improvement and in the phase-sensitive mode using Echo/Antiecho gradient selection, with multiplicity editing during selection step (States, Haberkorn, & Ruben, 1982). HMBC was optimized on long range coupling constants, with low-pass *J*-filter to suppress one-bond correlations, using gradient pulses for selection. HMBC was optimized for a 6 Hz coupling constant. The data matrix in all the heteronuclear experiments was extended to 2048 × 1024 points by using forward linear prediction extrapolation (Stern, Li, & Hoch, 2002).

2.5. Cell culture and samples preparations

A spontaneously transformed non-tumorigenic human keratinocyte cell line (HaCat cells) was used for *in vitro* scratch-wound-healing assay as reported by D'Agostino et al. (2015).

The lyophilized samples highlighted a water content of about 18% w/w for OPF and 17% w/w for both OSMF and ORE. The effect of these samples on wound closure rate was evaluated, incubating the scratched monolayer with OPF, ORE, OSMF at a final concentration of 0.1% w/v directly in the medium. Medium pH and osmolality (7,2–7,4 and 300 mosm) containing the diverse substances were verified to ensure physiological conditions.

2.6. Hydrodynamical characterization of Opuntia samples

The chromatographic analyses of *Opuntia* samples were performed using the SEC–TDA equipment by Viscotek (Lab Service Analytica, Italy) as previously described (La Gatta, De Rosa,

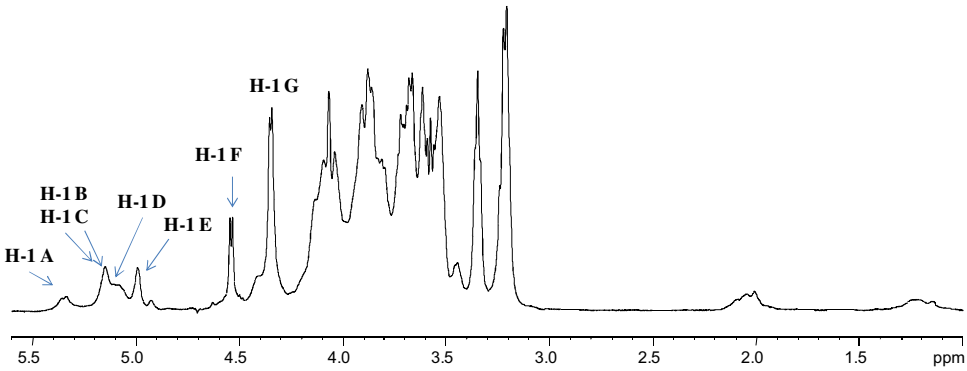

Fig. 1. ^{1}H NMR spectrum of digested product of OPF. Anomeric signals relative to each spin system (**A**-**G**) are indicated.

Marzaioli, Busico, & Schiraldi, 2010). Briefly, gel permeation chromatography (GPC) system was equipped with a triple detector consisting of an RI detector, a four-bridge viscosimeter (VIS), and an LS detector. This latter consisted of a right-angle light scattering (RALS) detector and an innovative low-angle light scattering (LALS) detector that performed measurements of the scattered light at 7° with respect to the incident beam with an optimum signal/noise. The OmniSEC software program was used for the acquisition and analysis of the Viscotek data. The *Opuntia* samples were analyzed at concentrations ranging from 0.3 to 4 g/L to have a column load for each analysis of approximately 0.2 dL and, at the same time, to also have appreciable LALS and intrinsic viscosity signals when analyzing low-molecular weight fragments. The dn/dc used is 0.146

The data obtained from viscotek analyses were: the molecular weight distribution (Mw), polydispersity (Mw/Mn), and intrinsic viscosity (IV).

2.7. In vitro *scratch wound healing assay*

Briefly, HaCat cells were grown until confluence in 12-multiwell culture plate, pre-coated with collagen and the monolayers were scratched mechanically with a sterile pipette tip (Ø = 0.1 mm). Uniformly sized wounds were produced of approximately 0.5–0.9 mm in width. Detached cells and debris were removed by PBS solution washing. The extracts (0.1% w/v) were added in DMEM 1% FBS solution. The experiment was performed in triplicate for each sample. The type of *in vitro* assay assisted by a time-lapse video microscopy station (TLVM) is described in details elsewhere (Jain, Worthylake, & Alahari, 2012).

The 'wound closure' phenomenon was monitored for 72–96 h using TLVM to observe on line the migration and eventually proliferation of HaCat cells to repair the wound, with and without the different treatments. The OKOLAB TLVM station allowed us to observe the reparation in different wells. In addition, quantitative analysis of wound healing was performed with OKO Vision software. The possibility to use 12-well plates into the stage incubator allowed to analyze simultaneously the diverse samples in triplicate respect to the control. For each well many view-fields were recorded overtime, thus an extensive and robust automatic analysis could be accomplished for 5–10 replicates of the specific condition analyzed. Taking into account that the height is fixed as it is the coordinate *y* of the field of view, we calculated the displacement of cellular front during the time using the simple equation: [(scratched area (μm^2)/height(μm))/2].

3. Results

3.1. *Purification and compositional analyses of* Opuntia *polysaccharide fraction (OPF)*

Compositional and absolute configuration analyses (De Castro et al., 2010; Leontein & Lönngren, 1978) were executed on an aliquot of the lyophilized OPF and were carried out by GLC–MS, indicating the presence of D-xylose, L-arabinose, D-galactose and D-glucose. Methylation analysis revealed the occurrence of terminal arabinofuranose, terminal xylopyranose, 5-substituted-arabinofuranose, 4-substituted-galactopyranose, 4-substituted-glucopyranose, 2,5-disubstituted-arabinofuranose, 3,5-disubstituted-arabinofuranose and 2,3,5-trisubstituted-arabinofuranose (see also NMR analysis below). The significant amount of 4-substituted-glucopyranose suggested the presence of a starch-like component, also evident from NMR preliminary analyses (Fig. S1), that was then removed by enzymatic treatment with α-amylase followed by extensive dialysis (cut-off 3500 Da). The starch-like constituent accounted for the 40% of the lyophilized **OPF** sample. Monosaccharide and methylation analyses repeated on digested OPF showed the absence of glucose, consistent with the removal of the starch-like component, and confirmed the presence of arabinose and xylose as the predominant sugars of OPF. Methylation data on the digested OPF product are summarized in Table S1.

The post amylase OPF underwent NMR experiments in order to define the structure of the polysaccharide component obtained from *Opuntia* cladodes.

3.2. *NMR spectroscopy analysis on OPF*

The ^{1}H NMR spectrum of digested product of OPF, reported in Fig. 1, showed the occurrence of a complex pattern of anomeric signals, seven identified as the main spin systems (**A**–**G**, Fig. 1 and Table 1). A combination of homo- and heteronuclear 2D NMR experiments were executed in order to assign all the spin systems and to define the monosaccharide sequence. In details, anomeric configuration of each monosaccharide was assigned on the basis of $^{3}J_{H1,H2}$ coupling constants and *intra*-residual NOE contacts whereas the relative configuration of each sugar unit was attributed based on vicinal $^{3}J_{H,H}$ values. Starting from anomeric proton signals, TOCSY and DQF-COSY spectra allowed the correct identification of all ring protons in parallel with the assignment of each carbon atom from analysis of the ^{1}H,^{13}C HSQC spectrum. Finally, both *inter*-residual NOE correlations (inferred from NOESY and ROESY experiments) and heteronuclear long-range correlations (detected in the ^{1}H,^{13}C

Table 1
^{1}H and ^{13}C (*italic*) chemical shifts (ppm) of OPF after enzymatic treatment with α-amylase.

Unit	1	2	3	4	5	6
A	5.33	4.09	4.18	4.14	3.77/3.69	
2,5-α-Ara*f*	108.3	82.5	82.6	82.3	66.9	
B	5.15	4.12	3.84	3.98	3.91	
5-α-Ara*f*	109.3	81.2	76.5	84.0	69.0	
C	5.14	4.10	3.83	4.01	3.80	
5-α-Ara*f*	109.0	81.1	76.5	84.0	69.1	
D	5.13	4.02	3.84	3.94	3.94	
3,5-α-Ara*f*	109.3	80.9	84.0	83.7	69.0	
E	4.98	4.02	3.90	4.02	3.71/3.57	
t- α-Ara*f*	107.3	82.1	76.7	84.0	63.2	
F	4.53	3.57	3.66	4.06	3.61	3.70
4-β-Gal*p*	104.2	71.7	73.1	77.3	74.6	60.6
G	4.35	3.20	3.35	3.52	3.87/3.22	
t-β-Xyl*p*	103.2	71.7	75.4	69.1	65.1	

HMBC spectrum) were pivotal to determine the primary sequence of monosaccharides in the OPF.

Interestingly, 2D NMR analysis suggested the presence of two different polysaccharide species pertaining to a branched arabinan-rich polysaccharide (as suggested by preliminary chemical analyses) and to a linear β-linked homopolymer. This latter was constituted by spin system **F** (H-1 at 4.53 ppm), attributed to a β-configured galactopyranose, as proven by its $^{1}J_{C1,H1}$ and $^{3}J_{H-1,H-2}$ values (163 and 8.0 Hz, respectively) and by the occurrence of an *intra*-residual NOE connectivity between H-1 and H-3/H-5 signals in the NOESY spectrum; finally, the observation of low $^{3}J_{H-3,H-4}$ and $^{3}J_{H-4,H-5}$ values (~3 Hz and 1 Hz respectively) was consistent with its *galacto*-configured nature. The low-field shift of C-4 of residue **F** highlighted a glycosylation site at this position. Thus, according to methylation data (Table S1), it was possible to ascertain the presence, as a component of the OPF, of an unbranched β-(1 → 4)-galactan polymer. As previously reported (Wefers, Tyl, & Bunzel, 2014), galactans composed of a β-(1 → 4)-linked backbone of galactopyranoses are frequently detected as main components of dicotyledonous plants. On the contrary, the second OPF polysaccharide constituent resulted in a complex and branched structure, composed of residues **A–E**, variously substituted by residue **G** (Table 1 and Fig. 1). In details, residue **G** was present as pyranose ring, according to either ^{13}C chemical shift values and the presence of long-range correlations between C-1/H-1 and H-5/C-5 in the ^{1}H,^{13}C HMBC spectrum.

Spin systems **A** (H-1 at 5.33 ppm), **B** (H-1 at 5.15 ppm), **C** (H-1 at 5.14 ppm), **D** (H-1 at 5.13 ppm) and **E** (H-1 at 4.98) were all α-arabinofuranosyl residues as proven by their $^{3}J_{H-1,H-2}$ (1.3–1.6 Hz) and $^{1}J_{C-1,H-1}$ (~170 Hz) values. They were present as furanose rings, as confirmed by downfield-shifted ring carbon signals (76–84.0 ppm) and by the *intra*-residual 1–4 correlations in the ^{1}H,^{13}C HMBC spectrum (Akiyama, Mori, & Kato, 1980). The identification of 5-linked, 2,5-linked, 3,5-linked and terminal α-arabinofuranosyl residues (Table 1) was further confirmed by comparison of carbon resonances with previously published data related to arabinofuranosides (Akiyama et al., 1980).

The ^{1}H,^{13}C HSQC spectrum (Fig. S2, Table 1) suggested the occurrence of an α-(1 → 5)-linked arabinofuranosyl chain as the main repeating unit of the polysaccharide core.

Spin system **G** (H-1 at 4.35 ppm) was assigned to a terminal β-xylose residue ($^{1}J_{C1,H-1}$ ~156 Hz), as shown by the large $^{3}J_{H,H}$ ring coupling constants (~9 Hz) and the H-5/C-5 diasterotopic methylene signals at δ_H 3.87-3.22 and δ_C 65.1 ppm. Moreover, the long-range correlation **G**1-**G**5 and the NOE contacts of H1 **G** with H5 **G** confirmed the xylopyranose nature of residue **G**.

The analysis of NOESY and ^{1}H,^{13}C HMBC spectra revealed the absence of correlations between the β-galactan polymer and the arabinan-rich polysaccharide, thus suggesting the existence of both components as separated entities. Unfortunately, any attempt to separate these two species failed.

The analysis of the NOESY spectrum revealed *inter*-residual NOE contacts between H-1 of 2,5-Ara*f* **A** and H-5 of 3,5-Ara*f* **D**. The former was, in turn, substituted at O-2 by terminal arabinose **E**, whereas residue 3,5-Ara*f* **D** was, in turn, substituted at O-3 by residue **C**, thus further suggesting the presence of contiguous branched arabinofuranose residues in the polysaccharide core. Further on, the H-1 of 3,5-Ara*f* residue **D** also showed an NOE contact with H-5 of residue 5-Ara*f* **B**. This latter was identified as composing the main (1 → 5)-linked arabinofuranose chain (Cardoso, Silva, & Coimbra, 2002). Owing to the huge overlapping of anomeric signals, relative intensities and, consequently, the lenght of such (1 → 5)-linked arabinofuranose repeating unit were difficult to exactly establish. Finally, the long-range correlation between H-1 of β-Xyl*p* **G** and C5 of 5-Ara*f* **C** at 69.1 ppm (Table 1) allowed to locate the terminal xylose **G** at position 5 of arabinose residues **C**: *t*-Xyl*p*-(1 → 5)-Ara*f*.

The linkage between *t*-Xyl and position 5 of arabinose residues **C** was further confirmed by selective chemical degradation, in fact a hydrofluoric acid (HF) treatment on an aliquot of the OPF completely depolymerized the acid labile arabinose glycosidic linkages. The ^{1}H and HMBC spectra of HF product are reported in Fig. 2, clearly showing the occurrence of a disaccharide made up of a reducing arabinose unit (both α- and β- anomers **Y** and **X** are indicated in Table S2 and Fig. 2) substituted at C-5 by a β-xylose residue (H-1 at 4.33 ppm, **Z** in Table S2 and Fig. 2), as demonstrated by the long-range correlation between H-1 of terminal xylose and C-5 of reducing (Table S2 and Fig. 2) arabinose residue.

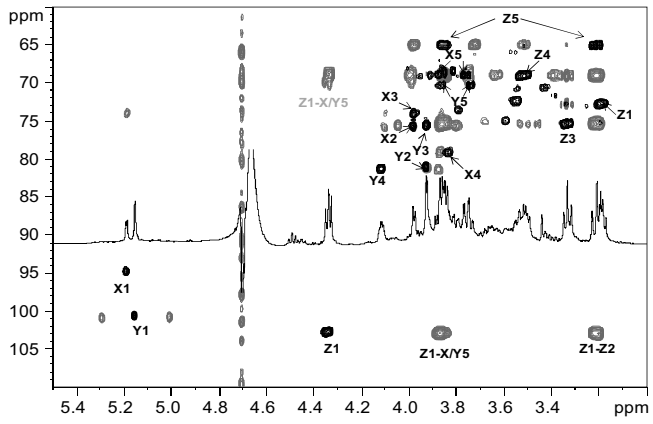

Fig. 2. Zoom of the overlapped ^{1}H, ^{13}C—HSQC (black) ^{1}H, ^{13}C—HMBC (grey) spectra of the HF hydrolysis product. The one-bond heteronuclear correlations and the long-range correlation between xylose (**Z**) and the arabinose residues (**X**/**Y**) were indicated.

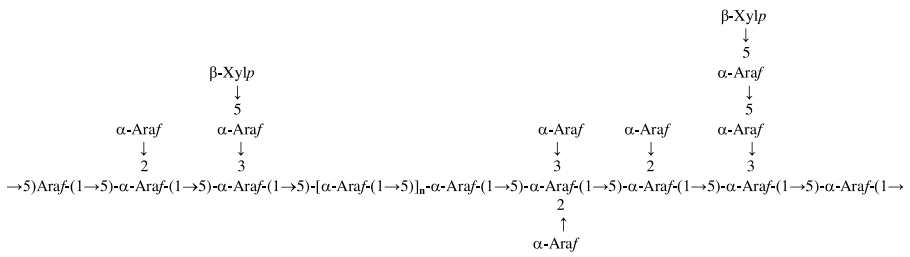

Fig. 3. Tentative structure for the xyloarabinan component of the OPF.

Therefore, combining NMR and chemical analyses, we propose for the arabinan component of the OPF a structure with a high degree of branching consisting of an α-(1 → 5)-linked arabinofuranosyl backbone with additional arabinofuranosyl residues located at O-2 and/or O-3 positions as previously described by Vignon, Heux, Malainine, and Mahrouzon (2004) free arabinans extracted from *Opuntia* cladodes spines and by Habibi et al. (2004, 2005) on free and pectic arabinans from prickly pear fruit peels. Intriguingly, none of the previous studies on *Opuntia* extracts reported, to date, the presence of xylose as part of the polysaccharide structure. Therefore, despite the general similarities with previously elucidated arabinan-rich polysaccharides (Habibi, Heyraud, Mahrouz, & Vignon, 2004; Habibi, Mahrouz, & Vignon, 2005), the presence of xylose units decorating, as capping groups, most of the polysaccharide side chains represents a peculiarity of *Opuntia* cladodes mucilage. The putative structure for the xyloarabinan costituent of the OPF is reported in Fig. 3; it just shows the different chemical possibilities in which Ara*f* can be involved in.

3.3. *Purification and NMR spectroscopy analyses of* Opuntia *small molecular weight fraction (OSMF)*

To determine the nature of the components of OSMF, a gel-filtration chromatography was executed. The size-exclusion chromatography yielded four main fractions, referred to here as OSMF **A**-**D** (not shown), that were collected, lyophilized and analyzed by a complete set of 1D and 2D NMR spectroscopy experiments. The ^{1}H NMR spectra of each fraction is reported in Fig. 4.

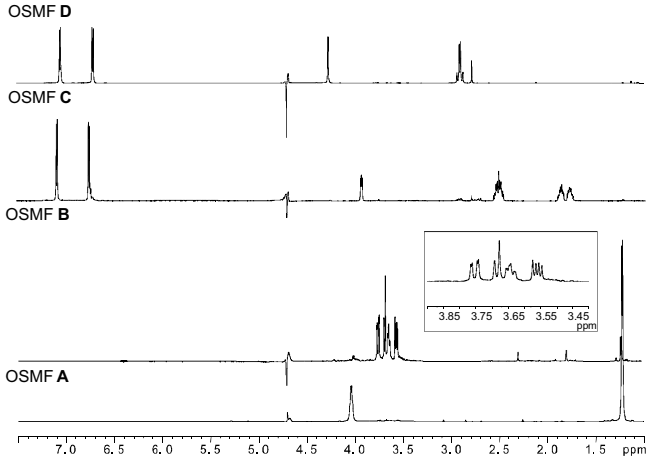

Fig. 4. ^{1}H NMR spectra of OSMF fractions obtained by gel filtration chromatography. In the inset a zoom of the signals relative to the polyol system representative of the OSMF fraction **B** is reported.

Fraction OSMF **A** (35%) was composed of lactic acid (Wishart et al., 2009), further confirmed by the observation of a long-range correlation of the oxymethine carbon atom (δ_H 4.08 ppm and δ_C

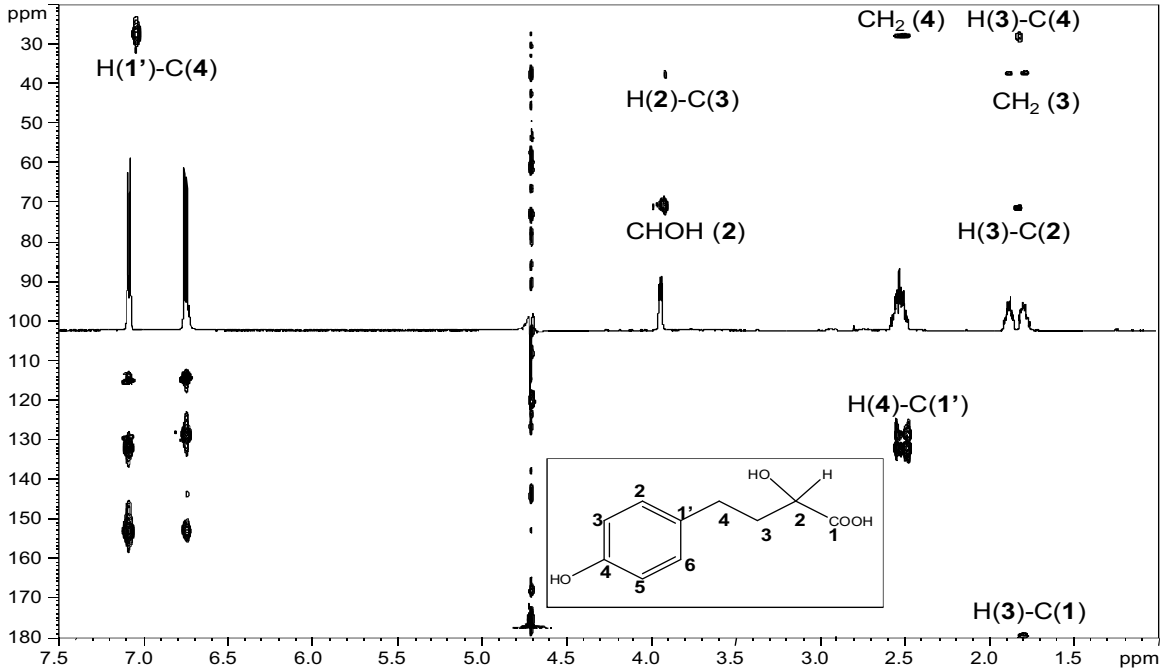

Fig. 5. Zoom of the overlapped ^{1}H,^{13}C HSQC and ^{1}H,^{13}C HMBC spectra of OSMF **C** fraction. The most relevant long-range correlations are reported. The structure of the 2-hydroxy-4-(4′-hydroxyphenyl)butanoic acid is sketched in the inset.

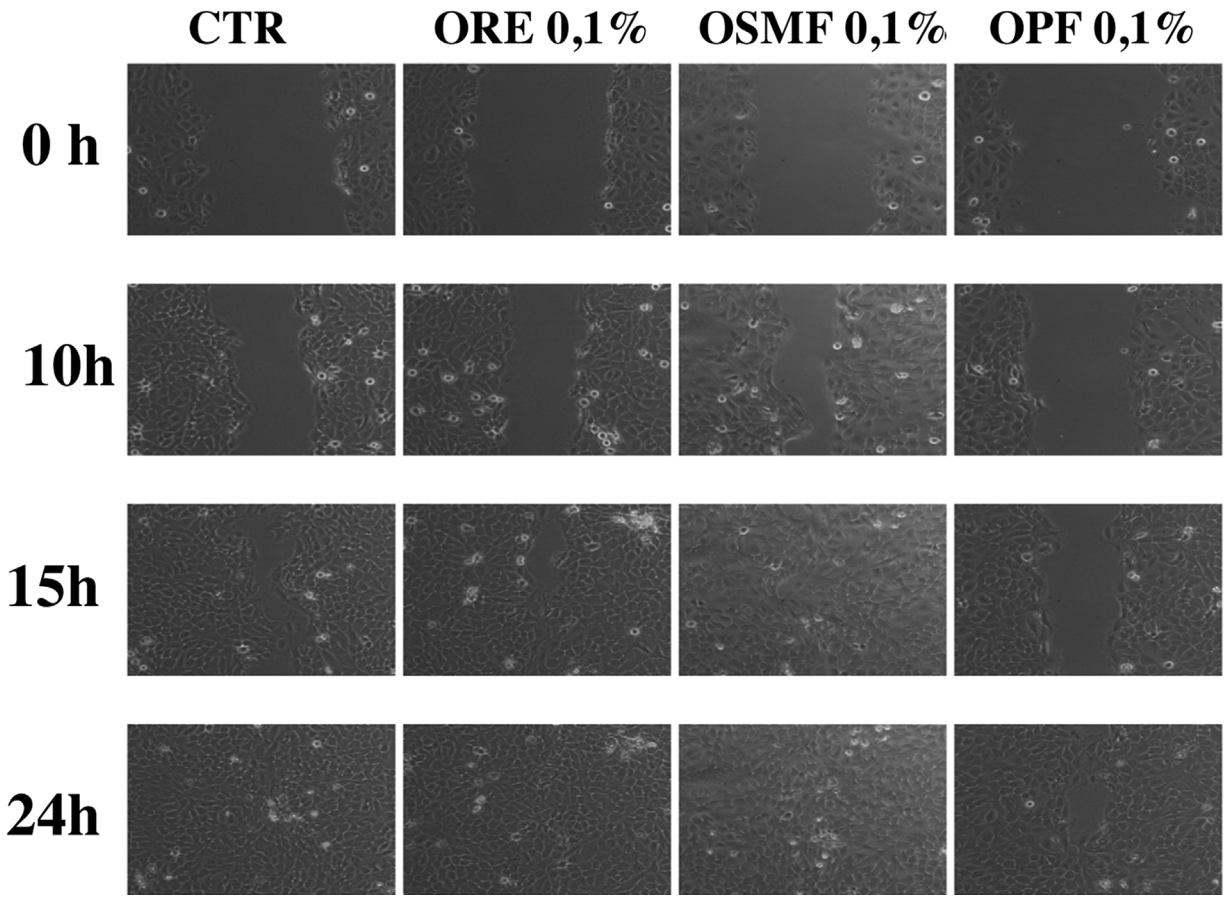

Fig. 6. Representative micrographs of HaCat scratched monolayer in time course of the experiments in the control and in the presence of treatments. Scale bar, 100 μm.

68.0 ppm, Table S3) with both the methyl and the carboxyl groups at δ_C 20.0 ppm and 179.5 ppm (Table S3) respectively. Accumulation of lactic acid is a common event occurring in plants that have undergone hypoxic or anoxic conditions due to the lactic fermentation; this latter is only apparently an un-physiological behavior since it was demonstrated that the lactate synthesis from malate is necessary to plants to ameliorate the cytoplasm pH conditions under hypoxia (Sakano, 1998).

Signals observed for fraction OSMF **B** (30%) were attributed to the D-mannitol (Popp & Smirnoff, 1995), a wide-spread hexitol found in plants as a fundamental intermediate in plant physiology although its biological role is not fully resolved (Collins & Ferrier, 1995; Gaidamauskas et al., 2005).

The nature of OSMF **B** was demonstrated by the presence, in the ^{13}C NMR spectrum (not shown), of three signals (resonating at 63.4, 69.2/70.7 ppm, Table S3), indicating a symmetric alditol; these signals were assigned to two oxymethylene and to four oxymethine carbon atoms respectively. This was further confirmed by comparison with literature data (Gallwey, Hawkes, Haycock, & Lewis, 1990; Popp & Smirnoff, 1995) and by the observation, in the $^{1}H,^{13}C$ HSQC spectrum (not shown), of correlations between H-1_a/H-6_a (3.75 ppm, Table S3) and H-1_b/H-6_b (3.56 ppm, Table S3) with the carbon atom resonance at 63.4 ppm (C-1/C-6) as well as the occurrence of correlation of signal at 3.64 ppm (relative to H-2 and 5) with the carbon atom resonating at 70.7 ppm (C-2/C-5) and the signal at 3.68 ppm (H-3 and 4) with the carbon resonance at 69.2 ppm (C-3/C-4).

1D and 2D NMR spectra executed on fraction OSMF **C** (20%) showed the typical signals relative to *para* substituted benzene residues and to a CH_2—CH_2—CHOH—COOH system. In details, in the ^{1}H NMR spectrum (Fig. 4), signals of two aromatic protons were detected at 6.75 ppm (2H, J = 8.2 Hz, H-3′/H-5′) and at 7.08 ppm (2H, J = 8.2 Hz, H-2′/H-6′). Signals relative to an oxymethine group were observed at 3.93 ppm (1H, J = 7.1 Hz, H-2); moreover, signals related to methylene groups at 1.85/1.77 ppm (position **3**, Fig. S3), 2.74/2.49 (position **4**, Fig. S3) were also clearly detectable. The $^{1}H,^{13}C$ HSQC spectrum (Fig. 5) confirmed the presence of six aromatic, two methylene and one oxymethine carbon atoms; moreover the $^{1}H,^{13}C$ HMBC spectrum (Fig. 5) highlighted the occurrence also of a carboxyl group. In this latter spectrum (Fig. 5), long-range correlations between the oxymethine carbon atom, the methylene group and the carboxylic acid group were detected. Further on, the aromatic carbon atom at 131.6 ppm (**1′**, Fig. 5) showed a long-range correlation with the methylene group at δ_C 29.9 ppm which, in turn, correlated with the other methylene group at δ_C 36.2 ppm, thus allowing to locate the sequence CH_2—CH_2—CHOH between the benzene ring and the carboxyl group. Finally, the downfield shift of the aromatic carbon atom (**4′**, Fig. 5) at 154.3 ppm confirmed the hypothesis of the occurrence of a hydroxyl group linked at such a position. Comparing with literature data on 3-hydroxy-5-(4′-hydroxyphenyl)pentanoic acid (Matsumoto, Hidaka, Nakayama, & Fukui, 1972; Miyase, Ueno, Takizawa, Kobayashi, & Oguchi, 1987) it was possible to establish the nature of such component of fraction OSMF **C** as a 2-hydroxy-4-(4′-hydroxyphenyl)butanoic acid (Fig. S3) whose presence was, to the best of our knowledge, never detected in *Opuntia* plants.

Fraction OSMF **D** (15%) was composed of two similar phenolic compounds whose chemical shifts assignment was in full agreement with previously reported data on piscidic and eucomic acids (Heller & Tamm, 1974; Mun'im, Negishi, & Ozawa, 2003; Sakamura, Yoshihara, & Toyoda, 1973; Stintzing & Carle, 2005; Takahira, Kusano, Shibano, Kusano, & Miyase, 1998; Yoshihara,

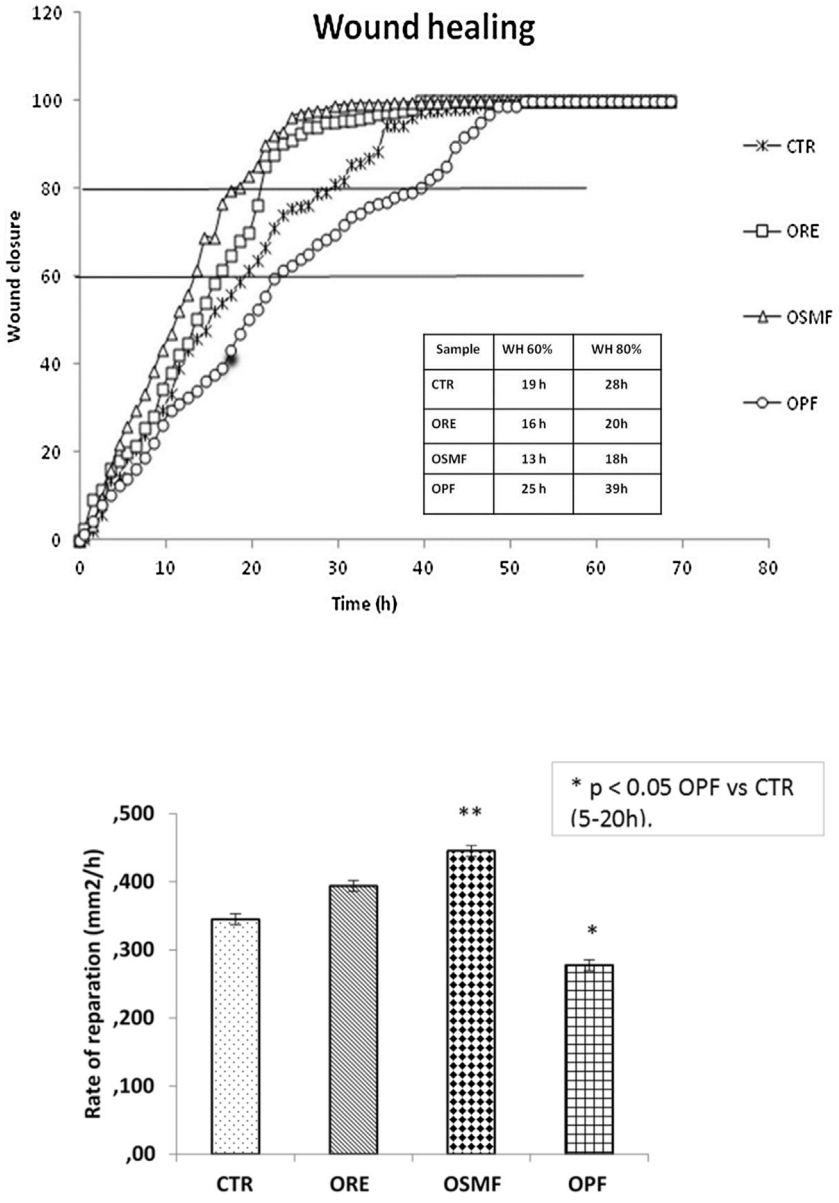

Fig. 7. (Top) Repair area percentage [as $\left(Areat_0 - Areat/Areat_0\right) x100$] for the control and in presence of the following stimuli: ORE, OPF, OSMF 0.1% w/v; the curves are averages of three different experiments with standard deviation within 5% of the value. (Bottom) Rate of reparation (mm^2/h) calculated as (Area $_{closure20\%}$- Area $_{closure60\%}$)/Δt with Δt representing the time range requested to run from 20% to 60% of closure. This Δt is 13,11,9,15 respectively for the control and in presence of ORE, OSMF and OPF.

Ichihara, Sakamura, 1971). The ring protons (H-2′, 5′, 6′, Fig. S3) were easily assigned on the basis of the typical *para* $J_{H,H}$ coupling pattern and the aliphatic system linked to the benzene ring was attributed via 2D NMR experiments, as stated above for fraction OSMF **C**. In details, signals related to piscidic acid in the ^1H NMR spectrum (Fig. 4) were detected at 7.04 ppm (2H, J = 8.2 Hz, H-2′/H-6′), 6.70 ppm (2H, J = 8.2 Hz, H-3′/H-5′), 2.90 ppm (2H, H-4) and 4.23 ppm (1H, H-2). The carbon atom chemical shifts values attained from the ^1H,^{13}C HSQC spectrum (not shown) and the long-range correlations detected in the ^1H,^{13}C HMBC spectrum (not shown) were also in accordance with reported data on piscidic acid (Takahira et al., 1998; Yoshihara et al., 1971). Owing to the overlap of signals relative to the aromatic ring and of the CH_2 group directly linked to the ring (**4**, Fig. S3), the occurrence of the eucomic acid was clarified by the observation of a further methylene-related signal at δ_H 2.78 ppm (2H, H-2) and δ_C at 45.0 ppm that showed to correlate with the carboxyl group at 174.0 ppm. As described elsewhere, piscidic and eucomic acids are rarely found in nature and are typical of CAM and succulence plants, with increment in their concentration with increasing age of the plants (Nordalh & Resser, 1966; Nordahl, Krogh, & Ogner, 1965) and were previously detected in *Opuntia* plants (Abdel-Hameed, Nagaty, Salman, & Bazaid, 2014; Stintzing & Carle, 2005).

3.4. *Viscotek analyses of* Opuntia *samples*

Hydrodynamic characterization of *Opuntia* samples, reported in Table S4, showed that ORE was composed of more species with a different molecular weight distribution, whereas the partially purified samples, the OPF and OSMF possessed respectively a high molecular (about 12,000 kDa) and very low molecular weight («4 kDa).

3.5. *Wound repairing capability of* Opuntia *samples*

The effect of *Opuntia* samples on scratched HaCat monolayer, was reported in Figs. 6 and 7. In particular, Fig. 7 reported a time course of representative fields of view of scratched monolayer in

the control wells and with the addition of the different fractions of the extracts. It was evident that ORE and OSMF increased the reparation respect to the control. On the contrary, OPF hampered the regeneration that naturally occurred in the control. This qualitative results were confirmed by the quantitative image analyses in the graphs of wound closure (area%) *vs* the time, reported in Fig. 7. The total reparation in presence of ORE and OSMF respectively occurred within 30 and 34 h, whilst the polysaccharide fraction led to a closure after 50 h, thus not improving the reparation rate respect to the control.

The slopes of the diverse curves were quite different. The 80% of closure occurred in 18 h for the OSMF, while at the same time the reparation in the presence of OPF was about 40%. Also the control curve is superior to OPF curve overall the time. ORE and OSMF showed a similar trend and rate. This can be explained by the preliminary observation that ORE is essentially constituted by OSMF for about 95%. The rate calculated between 20% and 60% of closure, that most represents the migration activity rather than the proliferation, confirmed the outcomes discussed above. Overall the assayed extracts improved the wound closure except for polysaccharide fraction that has a rate significantly ($P < 0.05$) lower compared to the control and to the other extracts.

Finally, cell migration, in terms of cells displacement in all the wells containing scratch HaCat monolayer, was also measured and reported in Fig. S4; these data confirmed a significant and greater displacement of cellular front in presence of OSMF and ORE, compared to OPF, both in the range 0–8 h and 8–18 h corresponding to a time-frame in which cell doubling is not relevant.

Thus, our data showed that whole ORE possesses a reparation curve (or wound healing) similar to OSMF, on the contrary OPF does not significantly contribute to skin repair. In view of these results, it is possible to suppose that the repairing effects of cladode mucilage is mainly attributable to the low molecular weight molecules.

4. Conclusions

Here we reported the complete structural characterization of the *Opuntia* mucilage constituents whose capability in repairing dermal tissue was also tested. The presence in mucilage of two main components differing in molecular weight distribution was highlighted by several steps of purifications. The high molecular weight component revealed to be composed of two polysaccharide entities: a linear β-(1 → 4)-galactose polymer and a highly branched xyloarabinan. On the other hand, a further purification step of the low molecular weight component revealed the presence of lactic acid, D-mannitol and three different phenolic compounds, two of which, the piscidic and the eucomic acids, are commonly detected in *Opuntia* plants; the third phenolic compound was identified as 2-hydroxy-4-(4′-hydroxyphenyl)butanoic acid that was never found in *Opuntia* plants. The effects on repairing dermal tissue of each *Opuntia* mucilage component was assessed through an *in vitro* scratched assay that resulted to be helpful in comparative assessing of the biorevitalizing effects of novel molecules or extracts. The results revealed that no particular capabilities in wound repairing is possessed by *Opuntia* cladodes polysaccharides. On the contrary, it is possible to conclude that a concerted action of the whole *Opuntia* mucilage, that is both the polysaccharide and the non-polysaccharide components, is responsible for the beneficial effects on dermal damages, with the main activity exerted by the non-polysaccharide constituents.

Thus, when topically applied, the *Opuntia* mucilage can produce a physical barrier on the cutis, protecting against stress factors, deeply hydrating skin and then favoring cutaneous reparative processes. Whether these properties are historically known, with the farmers of arid regions using the *Opuntia* cladodes juice as a natural gel to moisturize and heal cutis, on the other hand this is the first report of the clear elucidation of the structure and the related wound-healing properties of each *Opuntia* mucilage constituent. This represents an intriguing finding prompting to the future identification of the main component possessing the best repairing properties in a perspective of formulation of new bio-inspired cosmetic products such as anti-aging and wound-healing products for face and body.

Appendix A. Supplementary data

Supplementary data associated with this article can be found, in the online version, at http://dx.doi.org/10.1016/j.carbpol.2016.09.073.

References

Abdel-Hameed, E. S. S., Nagaty, M. A., Salman, M. S., & Bazaid, S. A. (2014). Phytochemicals, nutritionals and antioxidant properties of two prickly pear cactus cultivars (*Opuntia ficus indica* Mill.) growing in Taif, KSA. *Food Chemistry*, *160*, 31–38.

Akiyama, Y., Mori, M., & Kato, K. (1980). ^{13}C NMR analysis of hydroxyproline arabinosides from *Nicotiana tabacum*. *Agricultural and Biological Chemistry*, *44*, 2487.

Cardoso, S. M., Silva, A. M., & Coimbra, M. A. (2002). Structural characterisation of the olive pomace pectic polysaccharide arabinan side chains. *Carbohydrate Research*, *337*(10), 917–924.

Ciucanu, I., & Kerek, F. (1984). A simple and rapid method for the permethylation of carbohydrates. *Carbohydrates Research*, *131*, 209–217.

Collins, P. M., & Ferrier, R. J. (1995). *Monosaccharides: Their chemistry and their roles in natural products*. Chichester: Wiley.

D'Agostino, A., Stellavato, A., Busico, T., Papa, A., Tirino, V., Papaccio, G., et al. (2015). In vitro analysis of the effects on wound healing of high- and low-molecular weight chains of hyaluronan and their hybrid H-HA/L-HA complexes. *BMC Cell Biology*, *16*, 19.

De Castro, C., Parrilli, M., Holst, O., & Molinaro, A. (2010). Microbe-associated molecular patterns in innate immunity: Extraction and chemical analysis of gram-negative bacterial lipopolysaccharides. *Methods in Enzymology*, *480*, 89–115.

Gaidamauskas, E., Norkus, E., Vaiciūniene, J., Crans, D. C., Vuorinen, T., Jaciauskiene, J., et al. (2005). Evidence of two-step deprotonation of D-mannitol in aqueous solution. *Carbohydrate Research*, *340*(8), 1553–1556.

Galati, E. M., Monforte, M. T., Tripodo, M. M., d'Aquino, A., & Mondello, M. R. (2001). Antiulcer activity of *Opuntia ficus indica* (L.) Mill. (Cactaceae): Ultrastructural study. *Journal of Ethnopharmacology*, *76*, 1–19.

Galati, E. M., Pergolizzi, S., Miceli, N., Monforte, M. T., & Tripodo, M. M. (2002). Study on the increment of the production of gastric mucus in rats treated with *Opuntia ficus indica* (L.) Mill. cladodes. *Journal of Ethnopharmacology*, *83*(3), 229–233.

Gallwey, F. B., Hawkes, J. E., Haycock, P., & Lewis, D. (1990). ^{1}H NMR spectra and conformations of propane-1,2-diol, meso- and racemic butane-2,3-diols, and some alditols in non-aqueous media. *Journal of the Chemical Society Perkin Transactions*, *2*, 1979–1985.

Gescher, K., & Deters, A. M. (2011). *Typha latifolia* L. fruit polysaccharides induce the differentiation and stimulate the proliferation of human keratinocytes *in vitro*. *Journal of Ethnopharmacology*, *137*(1), 352–358.

Habibi, Y., Heyraud, A., Mahrouz, M., & Vignon, M. R. (2004). Structural features of pectic polysaccharides from the skin of *Opuntia ficus-indica* prickly pear fruits. *Carbohydrate Research*, *339*, 1119–1127.

Habibi, Y., Mahrouz, M., & Vignon, M. R. (2005). Arabinan-rich polysaccharides isolated and characterized from the endosperm of the seed of *Opuntia ficus-indica* prickly pear fruits. *Carbohydrate Polymers*, *60*, 319–329.

Heller, W., & Tamm, C. (1974). Isolierung, konstitution und synthese der (*R*)-(−)-Eucominsäure. *Helvetica Chimica Acta*, *57*, 1766–1784.

Jain, P., Worthylake, R. A., & Alahari, S. K. (2012). Quantitative analysis of random migration of cells using time-lapse video microscopy. *Journal of Visualized Experiments*, *63*, 3585.

Kaur, M., Kaur, A., & Sharma, R. (2012). Pharmacological actions of *Opuntia ficus indica*: a review. *Journal of Applied Pharmaceutical Science*, *02*(07), 15–18.

La Gatta, A., De Rosa, M., Marzaioli, I., Busico, T., & Schiraldi, C. (2010). A complete hyaluronan hydrodynamic characterization using a size exclusion chromatography-triple detector array system during in vitro enzymatic degradation. *Analytical Biochemistry*, *404*(1), 21–29.

Leontein, K., & Lönngren, J. (1978). Determination of the absolute configuration of sugars by Gas-Liquid Chromatography of their acetylated 2-octyl glycosides. *Methods in Carbohydrate Chemistry*, *62*, 359–362.

Matsumoto, T., Hidaka, K., Nakayama, T., & Fukui, K. (1972). The synthesis of configuration of fukiic acid derivatives. *Chemistry Letters*, *1*

Miyase, T., Ueno, A., Takizawa, N., Kobayashi, H., & Oguchi, H. (*1987*). Studies on the glycosides of *Epimedium grandiflorum* morr: Var. thunbergianum (Miq.) nakai. II. *Chemical and Pharmaceutical Bulletin*, *35*, 3713.

Mun'im, A., Negishi, O., & Ozawa, T. (2003). Antioxidative compounds from Crotalaria sessiliflora. *Bioscience, Biotechnology, and Biochemistry*, *67*(2), 410–414.
Nordalh, A., & Resser, D. (1966). The non-volatile acids of succulent plants exhibiting a marked diurnal oscillation in their acid content iii. the acids of *Kleinia repens* (L.) haw., begonia tuberhybrida (hort) and mesembryanthemum criniflorum L. fil. *Acta Chemica Scandinavica*, *20*, 2004–2007.
Nordalh, A., Krogh, A., & Ogner, G. (1965). Further observations on the occurrence of phorbic acid in plants. *Acta Chemica Scandinavica*, *19*, 1705–1708.
Parente, L. M., Lino Júnior Rde, S., Tresvenzol, L. M., Vinaud, M. C., de Paula, J. R., & Paulo, N. M. (2012). Wound healing and anti-Inflammatory effect in animal models of *Calendula officinalis* L.: Growing in Brazil. *Evidence-Based Complementary and Alternative Medicine*, *2012*, 375671.
Piantini, U., Sorensen, O. W., & Ernst, R. R. (1982). Multiple quantum filters for elucidating NMR coupling networks. *Journal of the American Chemical Society*, *104*, 6800–6801.
Pirbalouti, A. G., Azizi, S., Koohpayeh, A., & Hamedi, B. (2010). Wound healing activity of *Malva sylvestris* and *Punica granatum* in alloxan-induced diabetic rats. *Acta Poloniae Pharmaceutica Journal*, *67*(5), 511–516.
Popp, M., & Smirnoff, N. (1995). Polyol accumulation and metabolism during water deficit. In N. Smirnoff (Ed.), *Environment and Plant Metabolism: Flexibility and Acclimation* (pp. 199–215). Oxford: BIOS Scientific Publishers.
Rance, M., Sorensen, O. W., Bodenhausen, G., Wagner, G., Ernst, R. R., & Wuthrich, K. (1983). Improved spectral resolution in COSY (1)H NMR spectra of proteins via double quantum filtering. *Biochemical and Biophysical Research Communications*, *425*, 527–533.
Rizza, L., Frasca, G., Nicholls, M., Puglia, C., & Cardile, V. (2012). Caco-2 cell line as a model to evaluate mucoprotective proprieties. *International Journal of Pharmaceutics*, *422*(1–2), 318–322.
Sakamura, S., Yoshihara, T., & Toyoda, K. (1973). The constituents of *Petasites japonicus*: Structures of fukiic acid and fukinolic acid. *Agricultural and Biological Chemistry*, *37*, 1915–1921.
Sakano, K. (1998). Revision of biochemical pH-Stat: Involvement of alternative pathway metabolisms. *Plant and Cell Physiology*, *39*(5), 467–473.
Sepúlveda, E., Sáenz, C., Aliaga, E., & Aceituno, C. (2007). Extraction and characterization of mucilage in *Opuntia* spp. *Journal of Arid Enviroments*, *68*, 534–545.
States, D. J., Haberkorn, R. A., & Ruben, D. J. (1982). A two-dimensional nuclear Overhauser experiment with pure absorption phase in four quadrants. *Journal of Magnetic Resonance*, *8*, 286–292.
Stern, A. S., Li, K. B., & Hoch, J. C. (2002). Modern spectrum analysis in multidimensional NMR spectroscopy: Comparison of linear-prediction extrapolation and maximum-entropy reconstruction. *Journal of the American Chemical Society*, *124*, 1982–1993.
Stintzing, F. C., & Carle, R. (2005). Cactus stems (*Opuntia* spp.): A review on their chemistry: Technology and uses. *Molecular Nutrition & Food Research*, *49*(2), 175–194.
Takahira, M., Kusano, A., Shibano, M., Kusano, G., & Miyase, T. (1998). Constituents of *Cimicifuga* spp.: 24 Phenolics of Cimicifuga spp. 2. Piscidic acid and fukiic acid esters from Cimicifuga simplex. *Phytochemistry*, *49*, 2115–2119.
Trombetta, D., Puglia, C., Perri, D., Licata, A., Pergolizzi, S., Lauriano, E. R., et al. (2006). Effect of polysaccharides from *Opuntia ficus-indica* (L.) cladodes on the healing of dermal wounds in the rat. *Phytomedicine*, *13*, 352–358.
Vignon, M. R., Heux, L., Malainine, M. E., & Mahrouz, M. (2004). Arabinan-cellulose composite in *Opuntia ficus-indica* prickly pear spines. *Carbohydrate Research*, *339*(1), 123–131.
Wefers, D., Tyl, C. E., & Bunzel, M. (2014). Novel arabinan and galactan oligosaccharides from dicotyledonous plants. *Frontiers in Chemistry*, *2*, 100.
Wishart, D. S., Knox, C., Guo, A. C., Eisner, R., Young, N., Gautam, B., et al. (2009). HMDB: A knowledgebase for the human metabolome. *Nucleic Acids Research*, *37*(Database issue), D603–D610.
Yoshihara, T., Ichihara, A., Sakamura, S., & Senoh, S. (1971). The stereochemistry of fukiic acid and piscidic acid. *Tetrahedron Letters*, *41*, 3809–3812.